View metadata, citation and similar papers at core.ac.uk
brought to you by CORE
provided by PolyU Institutional Repository

A study on the disk-shaped piezoelectric transformer with multiple outputs

Mingsen Guo[a)]
Department of Physics, Wuhan University, Wuhan 430072, People's Republic of China and Department of Applied Physics and Materials Research Centre, The Hong Kong Polytechnic University, Hunghom, Kowloon, Hong Kong, People's Republic of China

K. H. Lam
Department of Applied Physics and Materials Research Centre, The Hong Kong Polytechnic University, Hunghom, Kowloon, Hong Kong, People's Republic of China

S. Wang
Department of Physics, Wuhan University, Wuhan 430072, People's Republic of China and Department of Applied Physics and Materials Research Centre, The Hong Kong Polytechnic University, Hunghom, Kowloon, Hong Kong, People's Republic of China

K. W. Kwok and Helen L. W. Chan
Department of Applied Physics and Materials Research Centre, The Hong Kong Polytechnic University, Hunghom, Kowloon, Hong Kong, People's Republic of China

X. Z. Zhao
Department of Physics, Wuhan University, Wuhan 430072, People's Republic of China

(Received 18 July 2007; accepted 6 November 2007; published online 7 December 2007)

In this study, a modified disk-shaped multiple-output piezoelectric transformer operated at the fundamental radial vibration mode has been presented. A derived equivalent circuit for the multioutput piezoelectric transformer was used to analyze the performance. Two piezoelectric transformers, a symmetrically electroded piezoelectric transformer with dual outputs and an asymmetrically electroded piezoelectric transformer with triple outputs, were fabricated with lead zirconate titanate piezoelectric ceramics. The characteristics of the two piezoelectric transformers were investigated experimentally. The piezoelectric transformer with multiple outputs has potential to be used in power supply units and other electronic circuits. © *2007 American Institute of Physics.* [DOI: 10.1063/1.2818809]

I. INTRODUCTION

Piezoelectric transducers have shown great promise as actuators and sensors because they are inexpensive, space efficient, lightweight, easily fabricated, and easily mounted on a variety of surfaces. With the development of fine ceramic technology, piezoelectric materials have been used for power devices, such as piezoelectric transformers and ultrasonic motors. A piezoelectric transformer is a device that transforms an ac voltage or current by the piezoelectric effect at electromechanical resonance frequency. Compared with an electromagnetic transformer, it has the following favorable characteristics: ease to be miniaturized with a large power to volume ratio; electromagnetic-noise-free; nonflammable because it has no windings; higher working frequency. Since the invention of the Rosen-type piezoelectric transformer,[1] many other types of piezoelectric transformer have been proposed and developed,[2–16] and some of them have been used in practice. In general, piezoelectric transformers are grouped into two classes: the first class (step-up transformer) has a voltage gain (=ratio of output voltage to input voltage) higher than one with a high output voltage of more than several hundred volts, mainly employed to power cold cathode fluorescent lamps for liquid crystal displays;[2] the second class (step-down transformer), with a voltage gain lower than 1 and a low output voltage of several volts, may be used as ac/dc and dc/dc adapters for power supplies.[6] However, almost all these piezoelectric transformers are designed with a single output. In many applications, for example, power supplies for portable equipment, the transformers with multiple outputs and small dimensions are needed to supply electric power to different parts in a system. This leads to a demand for piezoelectric transformers that can manage electric power and have several different outputs.

In this study, to widen the application range of piezoelectric transformers, modified disk-shaped piezoelectric ceramic transformers with dual or triple outputs were presented. The disk-shaped piezoelectric transformers were firstly proposed by Uchino's and co-workers for ac/dc and dc/dc adapter applications.[15–21] The design of the structure of the transformer is simple and stable. It operates at the fundamental radial vibration mode. The input and output electrodes were isolated from each other by insulating gaps. The input and output sections of the transformer were polarized along a thickness direction. Since the input and output sections have the same polarization direction, it is not easy to cause internal cracks during the electric poling process.[17,22,23]

[a)]Author to whom correspondence should be addressed; Electronic mail: gmsone_cn@hotmail.com

 © 2007 American Institute of Physics

Downloaded 10 Oct 2008 to 158.132.12.80. Redistribution subject to AIP license or copyright; see http://rsi.aip.org/rsi/copyright.jsp

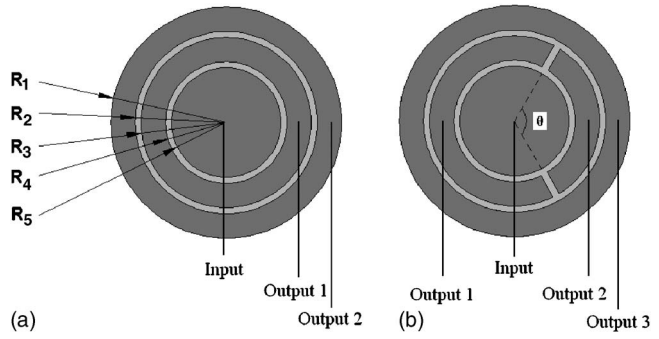

FIG. 1. Schematic diagram of piezoelectric transformers: (a) with dual outputs; (b) with triple outputs.

II. EXPERIMENTAL PROCEDURES

Figure 1 shows the construction of the piezoelectric transformers with dual outputs [Fig. 1(a)] and triple outputs [Fig. 1(b)]. The input and output electrodes are placed on the top surface of the ceramic. The inner disk electrode serves as input terminal, while the outer electrodes are output terminals. The bottom electrode (ground electrode), which is extended to the whole bottom surface of the disk, is common to both the input and output sections.

The active ceramic phase was lead zircodnate titanate (PZT) fabricated using PKI 802 PZT powder with a high mechanical quality factor ($Q_m > 900$). A PZT ceramic disk of radius $R_1 = 19.4$ mm and thickness $t = 1.9$ mm was fabricated by dry pressing and sintered at 1325 °C for 2 h. Silver slurry was screen printed on the ceramic disk and fired to form the patterned electrodes [Fig. 1(a)]. The sample with dual outputs (PT-A) was poled in silicone oil along the thickness direction by applying a dc field of 6 kV/mm at 120 °C for 30 min. Table I shows the dimensional specifications of fabricated piezoelectric transformers in this study. The measured properties of the PZT ceramics are shown in Table II.

Impedance properties of the piezoelectric transformer were measured as a function of frequency using an impedance analyzer (Agilent 4294A). The characteristics of the piezoelectric transformer under the variable load resistance were investigated using the experimental setup, as shown in Fig. 2. The piezoelectric transformer was driven by an ac signal generated by a function generator (AFG310, SONY Tektronix) and a high speed power amplifier (NF 4025, NF Corp.). In high-power experiments, a high-frequency electromagnetic transformer was used to amplify the voltage from the power amplifier. In Fig. 2, R_{L1}, R_{L2}, and R_{L3} are pure resistors. The voltage, current, and power of the input and output parts were measured by using digital oscilloscopes. The temperature rise of the transformer was measured by an infrared thermometer (KEYENCE IT2-50) about 10 min after applying the input voltage. After the characterization of the piezoelectric transformer with dual outputs (PT-A), a piezoelectric transformer (PT-B) with triple outputs was fabricated by dividing the electrode of the first output of PT-A into two parts ($\theta = 120°$) as shown in Fig. 1(b). The performance of PT-B was also evaluated with similar way as mentioned above.

TABLE I. Dimensional specifications of the piezoelectric transformers.

R_1 (mm)	R_2 (mm)	R_3 (mm)	R_4 (mm)	R_5 (mm)	t (mm)	θ (deg)
19.4	15.3	14.3	10.2	9.2	1.9	120

TABLE II. Measured properties of the PZT ceramics.

Density ρ ($\times 10^3$ kg/m^3)	7.6
Q_m	1500
$\varepsilon_{33}^T/\varepsilon_0$ at 1 kHz	1000
d_{33} ($\times 10^{-12}$ m/V)	150
d_{31} ($\times 10^{-12}$ m/V)	−65
Poisson's ratio σ^p	0.31
s_{11}^E ($\times 10^{-12}$ m^2/N)	10.4

III. RESULTS AND DISCUSSION

A. Equivalent circuit and its parameters

A multiterminal piezoelectric plate can be analyzed by tensor Green's function operations, Fourier-eigenmode expansions, and circuit-theory manipulations. Based on those analyses, the electrical equivalent circuit of the multioutput piezoelectric transformer can be derived in the vicinity of the resonance point.[24–26] The equivalent circuit of the dual-output piezoelectric transformer is shown in Fig. 3(a), it can be further simplified as shown in Fig. 3(b), in which $L_m = L_{m0}/A_{\text{input}}^2$, $C_m = C_{m0}A_{\text{input}}^2$, and $R_m = R_{m0}/A_{\text{input}}^2$ are the equivalent inductance, capacitance, and resistance, respectively; $C_{d,\text{input}}$, $C_{d,\text{out1}}$, and $C_{d,\text{out2}}$ are the clamped capacitances of the input, output 1, and output 2, respectively. The turn ratio of the ideal transformer N_1 and N_2 can be calculated by

$$N_1 = \frac{A_{\text{input}}}{A_{\text{out1}}} = \sqrt{\frac{L_{m,\text{out1}}}{L_{m,\text{input}}}}, \tag{1a}$$

$$N_2 = \frac{A_{\text{input}}}{A_{\text{out2}}} = \sqrt{\frac{L_{m,\text{out2}}}{L_{m,\text{input}}}}, \tag{1b}$$

where A_{input}, A_{out1}, and A_{out2} are the force factors of the input, output 1, and output 2, respectively.

The plate is driven into radial vibration by the application of an ac voltage. The differential equation for radial motion of the disk is[27]

$$c_{11}^p\left(\frac{\partial^2 u_r}{\partial r^2} + \frac{1}{r}\frac{\partial u_r}{\partial r} - \frac{u_r}{r^2}\right) = \rho\frac{\partial^2 u_r}{\partial t^2}, \tag{2}$$

where u_r is the radial component of displacement and

$$c_{11}^p = \frac{s_{11}^E}{(s_{11}^E)^2 - (s_{12}^E)^2}. \tag{3}$$

The pertinent constitutive equations are

$$T_{rr} = c_{11}^p\frac{\partial u_r}{\partial r} + c_{12}^p\frac{u_r}{r} - e_{31}^p E_3, \tag{4}$$

$$D_3 = e_{31}^p\frac{1}{r}\frac{\partial}{\partial r}(ru_r) + \varepsilon_{33}^p E_3, \tag{5}$$

where

Downloaded 10 Oct 2008 to 158.132.12.80. Redistribution subject to AIP license or copyright; see http://rsi.aip.org/rsi/copyright.jsp

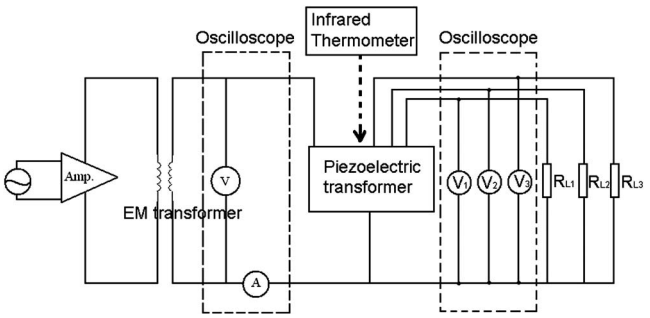

FIG. 2. Experimental setup for measuring the characteristics of the piezoelectric transformers.

$$c_{12}^{p} = \frac{-s_{12}^{E}}{(s_{11}^{E})^2 - (s_{12}^{E})^2}, \tag{6a}$$

$$e_{31}^{p} = \frac{d_{31}}{s_{11}^{E} + s_{12}^{E}}, \tag{6b}$$

$$\varepsilon_{33}^{p} = \frac{-2d_{31}^{2}}{s_{11}^{E} + s_{12}^{E}} + \varepsilon_{33}^{T}. \tag{6c}$$

Assuming the voltage applied to the input terminals of the disk-shaped piezoelectric transformer PT-A is $Ve^{i\omega t}$. The steady-state forced vibrational solution of Eq. (2) may be written in the form

$$u_r = AJ_1(\omega r/v^p)e^{i\omega t}, \tag{7}$$

where J_1 is the Bessel function of the first kind and first order, and

$$v^p = \sqrt{c_{11}^{p}/\rho}. \tag{8}$$

From Eq. (5), the input current is

$$I = \frac{\partial}{\partial t}\int_0^{R_5}\int_0^{2\pi} D_3 r dr d\theta = i\omega[-\varepsilon_{33}^{p}\pi R_5^2 E_3 + 2\pi R_5 u_r(R_5)]$$

$$= i\omega C_d V e^{i\omega t} + 2i\omega\pi e_{31}^{p} R_5 A J_1(\omega R_5/v^p)e^{i\omega t}, \tag{9}$$

where

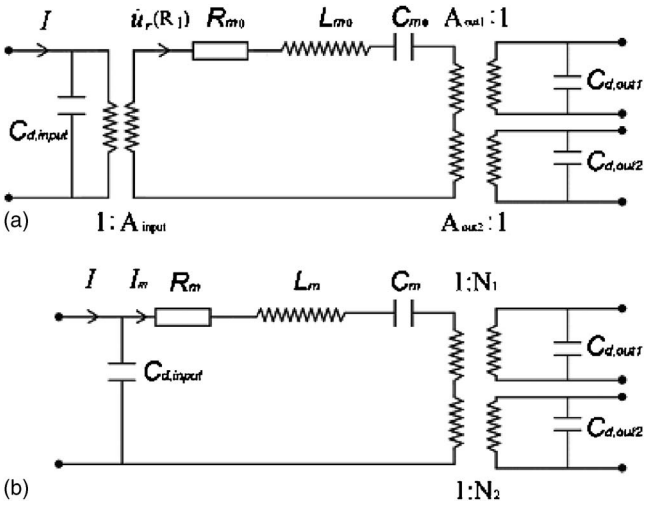

FIG. 3. Equivalent circuit of a dual-output piezoelectric transformer: (a) general form; (b) simplified form.

$$C_d = \pi R_5^2 \varepsilon_{33}^{p}/t = \varepsilon_{33}^{p} S/t. \tag{10}$$

From Eq. (9), the motional current I_m shown in Fig. 3(b) is

$$I_m = 2i\omega\pi e_{31}^{p} R_5 A J_1(\omega R_5/v^p)e^{i\omega t},$$

$$A_{\text{input}} = \frac{I_m}{\dot{u}_r(R_1)} = 2\pi e_{31}^{p} R_5 \frac{J_1(\omega R_5/v^p)}{J_1(\omega R_1/v^p)}. \tag{11}$$

The total kinetic energy of the disk is

$$E_K = \tfrac{1}{2}\rho\omega^2 \int\int\int u_r^2 dV$$

$$= \pi\omega^2 t\rho \int_0^{R_1} r[AJ_1(\omega r/v^p)e^{i\omega t}]^2 dr. \tag{12}$$

The resonance frequencies are given by the roots of the transcendental equation

$$\frac{(\omega R_1/v^p)J_0(\omega R_1/v^p)}{J_1(\omega R_1/v^p)} = 1 - \sigma^p, \tag{13}$$

where J_0 is the Bessel function of the first kind and zero order, and

$$\sigma^p = -s_{12}^{E}/s_{11}^{E} \tag{14}$$

is planar Poisson's ratio.

At resonance frequency of the fundamental radial vibration mode ω_r, the energy $L_m I_m^2/2$ stored in the equivalent inductance is equal to the total kinetic energy (output parts are short circuited). So we get

$$L_{m,\text{input}} = \frac{2E_K}{I_m^2} = \frac{t\rho\int_0^{R_1} r[J_1(\omega_r r/v^p)]^2 dr}{2\pi[e_{31}^{p} R_5 J_1(\omega_r R_5/v^p)]^2}. \tag{15}$$

By the same method, we have

$$L_{m,\text{out1}} = \frac{t\rho\int_0^{R_1} r[J_1(\omega_r r/v^p)]^2 dr}{2\pi(e_{31}^{p})^2[R_3 J_1(\omega_r R_3/v^p) - R_4 J_1(\omega_r R_4/v^p)]^2}, \tag{16a}$$

$$L_{m,\text{out2}} = \frac{t\rho\int_0^{R_1} r[J_1(\omega_r r/v^p)]^2 dr}{2\pi(e_{31}^{p})^2[R_1 J_1(\omega_r R_1/v^p) - R_2 J_1(\omega_r R_2/v^p)]^2}. \tag{16b}$$

The turn ratios are

$$N_1 = \frac{R_5 J_1(\omega_r R_5/v^p)}{R_3 J_1(\omega_r R_3/v^p) - R_4 J_1(\omega_r R_4/v^p)}, \tag{17a}$$

$$N_2 = \frac{R_5 J_1(\omega_r R_5/v^p)}{R_1 J_1(\omega_r R_1/v^p) - R_2 J_1(\omega_r R_2/v^p)}. \tag{17b}$$

The equivalent capacitance is

$$C_m = \frac{1}{\omega_r^2 L_m}. \tag{18}$$

The equivalent resistance can be calculated by

Downloaded 10 Oct 2008 to 158.132.12.80. Redistribution subject to AIP license or copyright; see http://rsi.aip.org/rsi/copyright.jsp

TABLE III. Calculated equivalent circuit parameters of the piezoelectric transformer, PT-A and PT-B.

	$L_{m,\text{input}}$ (mH)	$C_{m,\text{input}}$ (pF)	$R_{m,\text{input}}$ (Ω)	$C_{d,\text{input}}$ (pF)	N_1	N_2	N_3	$C_{d,\text{out1}}$ (pF)	$C_{d,\text{out2}}$ (pF)	$C_{d,\text{out3}}$ (pF)
PT-A	86.1	73.9	22.7	1074	1.21	1.67	⋯	1274	1805	⋯
PT-B	86.1	73.9	22.7	1074	1.82	3.64	1.67	849	425	1805

$$R_m = \frac{\omega_r L_m}{Q_m}. \tag{19}$$

The calculated equivalent circuit parameters of PT-A are shown in Table III. The dimensions in Table I, and the material properties in Table II, are taken for calculation.

The voltage gain of the transformer can be derived by transferring the output side of the equivalent circuit to the input side and analyzing the circuit:

$$\frac{V_{\text{out1}}}{V_{in}} = \frac{1}{N_1}\left\{\left[R_m + \frac{R_{L1}}{N_1^2(1+\omega^2 C_{d,\text{out1}}^2 R_{L1}^2)} + \frac{R_{L2}}{N_2^2(1+\omega^2 C_{d,\text{out2}}^2 R_{L2}^2)}\right]^2 + \left[\omega L_m - \frac{1}{\omega C_m} - \frac{R_{L1}^2 \omega C_{d,\text{out1}}}{N_1^2(1+\omega^2 C_{d,\text{out1}}^2 R_{L1}^2)} - \frac{R_{L2}^2 \omega C_{d,\text{out2}}}{N_2^2(1+\omega^2 C_{d,\text{out2}}^2 R_{L2}^2)}\right]^2\right\}^{-1/2} \times \left(\frac{1}{R_{L1}^2} + \omega^2 C_{d,\text{out1}}^2\right)^{-1/2}, \tag{20a}$$

$$\frac{V_{\text{out2}}}{V_{in}} = \frac{1}{N_2}\left\{\left[R_m + \frac{R_{L1}}{N_1^2(1+\omega^2 C_{d,\text{out1}}^2 R_{L1}^2)} + \frac{R_{L2}}{N_2^2(1+\omega^2 C_{d,\text{out2}}^2 R_{L2}^2)}\right]^2 + \left[\omega L_m - \frac{1}{\omega C_m} - \frac{R_{L1}^2 \omega C_{d,\text{out1}}}{N_1^2(1+\omega^2 C_{d,\text{out1}}^2 R_{L1}^2)} - \frac{R_{L2}^2 \omega C_{d,\text{out2}}}{N_2^2(1+\omega^2 C_{d,\text{out2}}^2 R_{L2}^2)}\right]^2\right\}^{-1/2} \times \left(\frac{1}{R_{L2}^2} + \omega^2 C_{d,\text{out2}}^2\right)^{-1/2}. \tag{20b}$$

For the triple-output piezoelectric transformer PT-B as shown in Fig. 1(b), the equivalent inductances of outputs 1 and 2 are

$$L_{m,B\text{out1}} = \left(\frac{2\pi}{2\pi - \theta}\right)^2 L_{m,A\text{out1}}, \tag{21a}$$

$$L_{m,B\text{out2}} = \left(\frac{2\pi}{\theta}\right)^2 L_{m,A\text{out1}}. \tag{21b}$$

The calculated results are also shown in Table III. Based on the results, the impedance characteristics, voltage gain, and efficiency of the piezoelectric transformer can be calculated.[24]

B. PT-A with dual outputs

The symmetrically electroded piezoelectric transformer, PT-A, is expected to have good resonance state free from any spurious vibration mode. The measured impedance spectra of the input part of PT-A are shown in Fig. 4. The equivalent circuit parameters of the input impedance of PT-A were measured using an impedance analyzer, the results are shown in Table IV. The impedance spectra of output parts (not shown here) were also measured and the equivalent circuit parameters are listed in Table IV. During the measurement, each part was tested under the condition that the other parts were short circuited, so that an equivalent circuit of the dual-output piezoelectric transformer connected with load resistances can be obtained [Fig. 3(b)].[9,24] The measured turn ratios N_1 and N_2 of PT-A at the fundamental radial vibration mode are 1.12 and 1.70, respectively. It shows that the theoretical results are in agreement with the experimental ones.

It is known that the efficiency of a piezoelectric transformer attains a maximum value when the load resistance is equal to $1/\omega C_{d,\text{output}}$, where $C_{d,\text{output}}$ is the clamped capacitance of the output part.[9] This load is called the matching load. For PT-A, matching loads are $R_{L1}=1.3$ kΩ, $R_{L2}=1.1$ kΩ. Figure 5 shows the frequency dependence of the voltage gain and the efficiency of PT-A with the matching loads. During the measurement, the input voltage was 50 V_{pp}, the temperature rise of the piezoelectric transformer was below 5 °C. The voltage gains of the output 1 and the output 2 simultaneously attain their maximum values of 1.17 and 0.69, respectively, at 62.7 kHz. A maximum efficiency of 98% was obtained at 63.6 kHz. In the frequency range of 61.9–64.9 kHz, the efficiency was higher than 90%.

Figure 6 shows the load resistance dependence of the maximum voltage gain of PT-A. Here, the maximum voltage gain means the maximum value of an output with respect to the driving frequency. During the measurements, the tested output part was connected with a variable resistor, while the

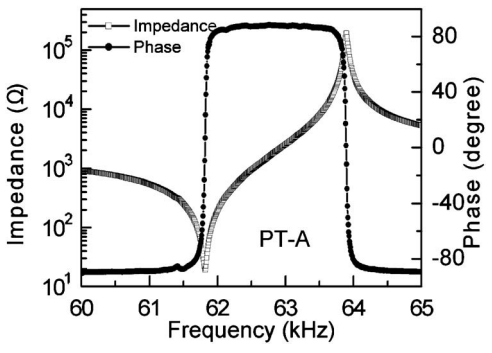

FIG. 4. The impedance spectra of the input part of PT-A near the resonance frequency of the fundamental radial vibration mode.

Downloaded 10 Oct 2008 to 158.132.12.80. Redistribution subject to AIP license or copyright; see http://rsi.aip.org/rsi/copyright.jsp

TABLE IV. Measured equivalent circuit parameters of input and output parts of the piezoelectric transformers, PT-A and PT-B.

	f_r (kHz)	f_a (kHz)	R_m (Ω)	L_m (mH)	C_m (pF)	C_d (pF)	Q_m
PT-A (dual outputs)							
Input	61.82	63.89	18.75	74.93	88.47	1292	1550
Output 1	61.82	62.91	23.28	94.27	70.33	1962	1570
Output 2	61.83	62.24	53.40	217.8	30.42	2282	1580
PT-B (triple outputs)							
Input	61.98	64.03	19.38	77.32	85.31	1261	1550
Output 1	61.99	62.67	54.01	221.5	29.77	1332	1600
Output 2	61.98	62.32	209.0	841.0	7.843	696.2	1570
Output 3	61.98	62.38	59.10	229.2	28.77	2202	1510

other output part was matching loaded. It is seen that the maximum voltage gains of the two output parts increase with the load resistance. When the load resistances are 0.1 and 100 kΩ, the maximum voltage gains of the output 1 are 0.32 and 4.41, respectively, and for the output 2, the maximum voltage gains are 0.13 and 1.29, respectively.

To investigate the effect of the load of one output on the voltage gains of the other outputs, the relationship between the voltage gain of the output 1 (or 2) and the operating frequency was measured for PT-A when its output 2 (or 1) was short circuited, open circuited, and matching loaded, respectively. As shown in Fig. 7, the voltage gain of one output is affected by the load of the other output. The maximum voltage gain of one output and its corresponding frequency change with the load of the other output. The equivalent circuit shown in Fig. 3 can be used to explain these characteristics (the simulated results are not shown here). Since transformers with constant voltage gains are preferred in practical applications, the interaction of loads between the output parts should be considered.

The relationship among the maximum output power, temperature rise, and input voltage of PT-A at the fundamental radial vibration mode with matching loads is shown in Fig. 8. The maximum output power is defined as the maximum value of the output power with respect to the driving frequency for a given input voltage. The temperature rise of the transformer was measured at the inner annular gap where no electrode exists and the temperature is the highest. It is seen that a maximum output power of 17.2 W (P_{out1}=12.1 W, P_{out2}=5.1 W) can be obtained with a temperature rise of 12 °C at an input voltage of 300 V_{pp}.

C. PT-B with triple outputs

The output 1 and the output 2 of PT-B with matching loads are expected to have identical output voltages. The ratio of the output power of output 1 to that of output 2 is expected as

$$P_{out1}/P_{out2} = (2\pi - \theta)/\theta = 2. \quad (22)$$

The measured impedance spectra of the input part of PT-B are shown in Fig. 9. The resonance and antiresonance responses of the fundamental radial vibration mode are clear. A spurious vibration mode at frequency about 63.3 kHz may be due to the asymmetrical electrode patterns of outputs 1 and 2. The equivalent circuit parameters of the input and output parts of PT-B are listed in Table IV. The measured turn ratios N_1, N_2, and N_3 of PT-B at the fundamental radial vibration mode are 1.69, 3.30, and 1.72, respectively. The matching loads are R_{L1}=1.9 kΩ, R_{L2}=3.7 kΩ, R_{L3}=1.1 kΩ. Figure 10 shows the frequency dependence of voltage gain of PT-B with the matching loads. The voltage gains of the outputs 1, 2, and 3 simultaneously attain their maximum values of 1.14, 1.13, and 0.72, respectively at 62.8 kHz. The relationship between the maximum output power, temperature rise, and input voltage of PT-B at the fundamental radial vibration mode with the matching loads is shown in Fig. 11. A maximum output power of 16.7 W (P_{out1}=7.7 W,

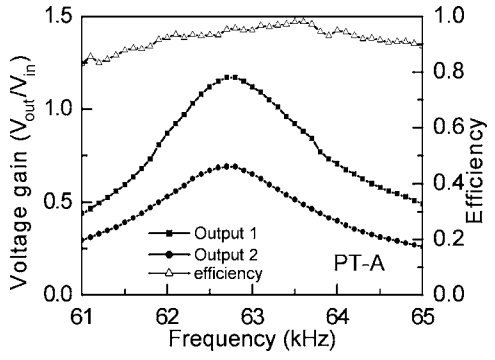

FIG. 5. Frequency dependence of the voltage gains and efficiency of PT-A with the matching loads.

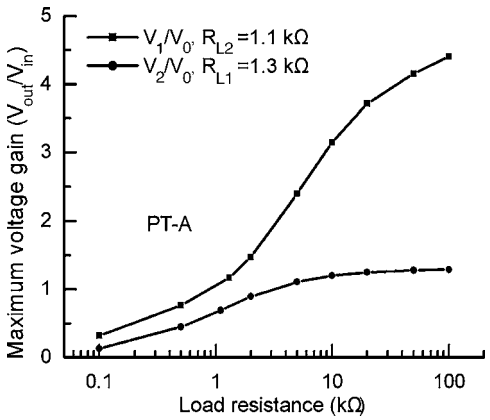

FIG. 6. Load resistance dependence of the maximum voltage gain of PT-A.

Downloaded 10 Oct 2008 to 158.132.12.80. Redistribution subject to AIP license or copyright; see http://rsi.aip.org/rsi/copyright.jsp

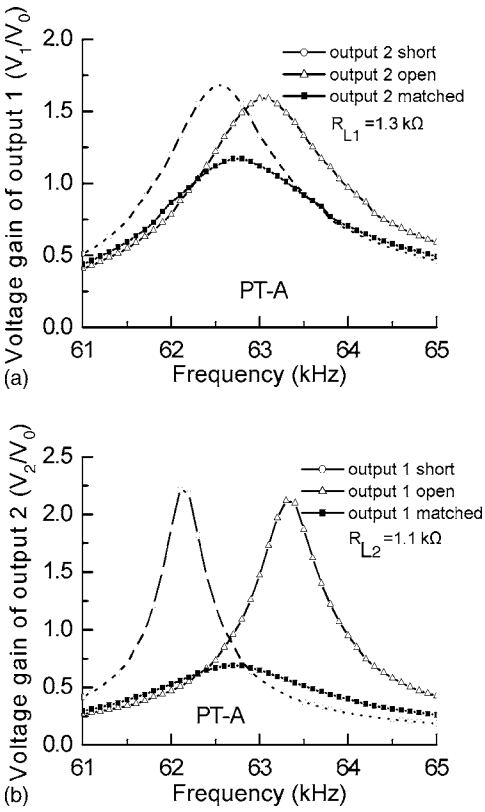

FIG. 7. Relationship between the voltage gain of (a) output 1, (b) output 2, and the frequency of PT-A when the other output is short circuited, open circuited, and matching loaded, respectively.

P_{out2}=3.8 W, P_{out3}=5.2 W) can be obtained with a temperature rise of 13 °C at an input voltage of 300 V_{pp}.

As shown in the experimental results, the voltage gains of the piezoelectric transformer with multiple outputs depend on the driving frequency, load resistances, piezoelectric material properties, and dimensions of the electrodes. In addition, by making the input and/or output portions into multilayer structures, the voltage gains of the piezoelectric transformer can be easily tuned. The equivalent circuit (e.g., Fig. 3 for dual-output piezoelectric transformer) related to material coefficients and dimension parameters of electrodes can be used to simulate the performance of the piezoelectric transformer in low power conditions. Numerical analysis based on finite-element method is also useful for handling

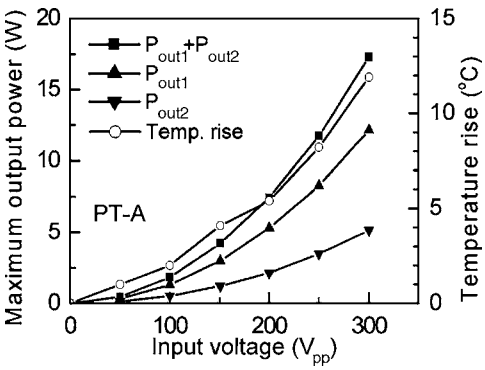

FIG. 8. Relationship among the maximum output power, temperature rise, and input voltage of PT-A with the matching loads.

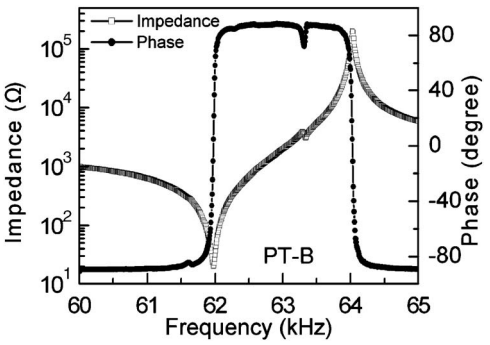

FIG. 9. The impedance spectra of the input part of PT-B near the resonance frequency of the fundamental radial vibration mode.

the complicated geometry of real device structures and electrode patterns. The power-to-volume ratio is important for reducing the size of power supply units. When driven under high fields, heat generation in the piezoelectric transformer may be the most important keypoint of structural degradation or even failure. To increase the power-to-volume ratio, a good design of structure and excellent piezoelectric ceramics with high-power density is needed.[8]

IV. SUMMARY

The modified disk-shaped, multiple-output piezoelectric transformer operated at the fundamental radial vibration mode has been presented. A derived equivalent circuit for the multioutput piezoelectric transformer was used to analyze the performance. Two piezoelectric transformers, a symmetrically electroded piezoelectric transformer with dual outputs (PT-A), and an asymmetrically electroded piezoelectric transformer with triple outputs (PT-B) were fabricated with PZT piezoelectric ceramics. The features of the two piezoelectric transformers have been illustrated. For PT-A with the matching loads, the voltage gains of outputs 1 and 2 are 1.17 and 0.69, respectively. A maximum output power of 17.2 W (12.1 W in output 1 and 5.1 W in output 2) can be obtained with a temperature rise of 12 °C at an input voltage of 300 V_{pp}. For PT-B, the voltage gains of the outputs 1, 2, and 3 are 1.14, 1.13, and 0.72, respectively. A maximum output power of 16.7 W (7.7 W in output 1, 3.8 W in output 2, and 5.2 W in output 3) can be obtained with a temperature

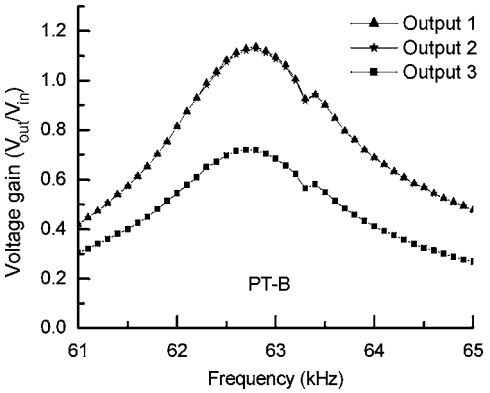

FIG. 10. Frequency dependence of the voltage gains of PT-B with the matching loads.

Downloaded 10 Oct 2008 to 158.132.12.80. Redistribution subject to AIP license or copyright; see http://rsi.aip.org/rsi/copyright.jsp

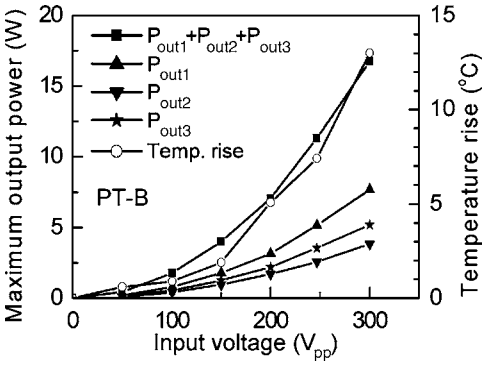

FIG. 11. Relationship among the maximum output power, temperature rise, and input voltage of PT-B with the matching loads.

rise of 13 °C at an input voltage of 300 V_{pp}. The piezoelectric transformer with multiple outputs has potential to be used in power supply units and other electronic circuits.

ACKNOWLEDGMENTS

This work was supported by the Niche Area Project (No. 1-BB95) and the Centre for Smart Materials of The Hong Kong Polytechnic University.

[1] C. A. Rosen, K. A. Fish, and H. C. Rothenberg, U.S. Patent No. 2830274 (8 April 1958).
[2] S. Kawashima, O. Ohnishi, H. Hakamata, S. Tagami, A. Fukuoka, T. Inoue, and S. Hirose, Proc.-IEEE Ultrason. Symp. **1**, 525 (1994).
[3] Y. Fuda, K. Kumasaka, M. Katsuno, H. Sato, and Y. Ino, Jpn. J. Appl. Phys., Part 1 **36**, 3050 (1997).
[4] Y. Sasaki, M. Yamamoto, A. Ochi, T. Inoue, and S. Takahashi, Jpn. J. Appl. Phys., Part 1 **38**, 5598 (1999).
[5] K. Nakamura and Y. Adachi, Electron. Commun. Jpn., Part III: Fundamental Electronic Science **81**, 1 (1998).
[6] O. Ohnishi, H. Kishie, A. Iwamoto, Y. Sasaki, T. Zaitsu, and T. Inoue, Proc.-IEEE Ultrason. Symp. **1**, 483 (1992).
[7] M. Yamamoto, Y. Sasaki, A. Ochi, T. Inoue, and S. Hamamura, Jpn. J. Appl. Phys., Part 1 **40**, 3637 (2001).
[8] J. H. Hu, Y. Fuda, M. Katsuno, and T. Yoshida, Jpn. J. Appl. Phys., Part 1 **38**, 3208 (1999).
[9] J. H. Hu, H. L. Li, Helen L. W. Chan, and C. L. Choy, Sens. Actuators, A **88**, 79 (2001).
[10] J. L. Du, J. H. Hu, and K. J. Tseng, IEEE Trans. Ultrason. Ferroelectr. Freq. Control **51**, 502 (2004).
[11] E. M. Baker, W. Huang, D. Y. Chen, and F. C. Lee, IEEE Trans. Power Electron. **20**, 1213 (2005).
[12] K. Nakamura and K. Kumasaka, Proc.-IEEE Ultrason. Symp. **2**, 999 (1995).
[13] M. Ueda, M. Satoh, S. Ohtsu, and N. Wakatsuki, Proc.-IEEE Ultrason. Symp. **2**, 977 (1992).
[14] S. K. Kim and Y. H. Seo, Appl. Phys. Lett. **88**, 263510 (2006).
[15] K. Uchino, B. Koc, P. Laoratanakul, and A. V. Carazo, Ferroelectrics **263**, 1391 (2001).
[16] A. V. Carazo and K. Uchino, J. Electroceram. **7**, 197 (2001).
[17] P. Laoratanakul, A. V. Carazo, P. Bouchilloux, and K. Uchino, Jpn. J. Appl. Phys., Part 1 **41**, 1446 (2002).
[18] H. W. Kim, S. X. Dong, P. Laoratanakul, K. Uchino, and T. G. Park, IEEE Trans. Ultrason. Ferroelectr. Freq. Control **49**, 1356 (2002).
[19] S. Manuspiya, P. Laoratanakul, and K. Uchino, Ultramicroscopy **41**, 83 (2003).
[20] S. Priya, S. Ural, H. W. Kim, K. Uchino, and T. Ezaki, Jpn. J. Appl. Phys., Part 1 **43**, 3503 (2004).
[21] S. Priya, H. Kim, S. Ural, and K. Uchino, IEEE Trans. Ultrason. Ferroelectr. Freq. Control **53**, 810 (2006).
[22] K. Uehara, T. Inoue, A. Iwamoto, O. Ohnishi, and Y. Sasaki, U.S. Patent No. 5278471 (11 January 1994).
[23] M. S. Guo, D. M. Lin, K. H. Lam, S. Wang, H. L. W. Chan, and X. Z. Zhao, Rev. Sci. Instrum. **78**, 035102 (2007).
[24] J. L. Du, J. H. Hu, K. J. Tseng, C. S. Kai, and G. C. Siong, IEEE Trans. Ultrason. Ferroelectr. Freq. Control **53**, 579 (2006).
[25] W. P. Mason, *Piezoelectric Crystals and Their Application to Ultrasonics* (Van Nostrand, Princeton, NJ, 1950).
[26] R. Holland, J. Acoust. Soc. Am. **41**, 940 (1967).
[27] ANSI/IEEE Std. 176–1987, *IEEE Standard on Piezoelectricity* (IEEE, New York, 1987).

Downloaded 10 Oct 2008 to 158.132.12.80. Redistribution subject to AIP license or copyright; see http://rsi.aip.org/rsi/copyright.jsp